References

[1] Kerrebrock, J L, "Conduction in gases with elevated electron temperature," *Engineering Aspects of Magnetohydrodynamics* (Columbia University Press, New York, 1962), p 327; also "Non-equilibrium effects on conductivity and electrode heat transfer in ionized gases," Daniel and Florence Guggenheim Jet Propulsion Center California Institute of Technology, TN 4 (November 1960)

[2] Karlowitz, B and Halasz, D, U S Patent 2 210,918 (August 13, 1940)

[3] Chapman, S and Cowling, T G, *The Mathematical Theory of Non Uniform Gases* (Cambridge University Press, New York, 1958), Chap 8

[4] Massey, H S W and Burhop, E H S, *Electronic and Ionic Impact Phenomena* (Oxford University Press, New York 1956), p 279

[5] Ben Daniel, D J and Tamor, S, "Theory of nonthermal ionization in cesium discharges, Phys Fluids **5**, 500 (1962)

[6] Byron, S, Bortz, P, and Russell, G, 'Electron-ion reaction rate theory: determination of the properties of non equilibrium monatomic plasmas in M H D generators and accelerators and in shock tubes" Fourth Symposium on Engineering Aspects of Magnetohydrodynamics, Univ of California (April 10–11 1963)

[7] Gryzinski, M, Classical theory of electronic and ionic inelastic collisions, Phys Rev **115**, 374 (1959)

[8] Lutz, M 'Radiant energy loss from a cesium-argon plasma to an infinite plane parallel enclosure," Avco Everett Research I ab, Res Rept 175 (September 1963)

[9] Hurwitz, H, Jr, Kilb, R W, and Sutton, G W J Appl Phys **32** (February 1961)

[10] Oates, G C, Richmond, J K, Aoki, Y, and Grohs, G, "Loss mechanisms of a low temperature plasma accelerator,' ARS J **32**, 541 (1962)

[11] Hale, F J and Kerrebrock, J L, "Insulator boundary layers in magnetohydrodynamic channels," AIAA J **2**, 461 1964)

[12] Smith, J M, "Theory of length required to reach the state of non equilibrium in an MHD generator, Fourth Symposium on Engineering Aspects of Magnetohydrodynamics, Univ of California (April 10–11 1963)

[13] Wright J K, 'A temperature instability in magnetohydrodynamic flow," Proc Phys Soc **81**, 498 (1963)

[14] Hinnov, E and Hirschberg, J G, "Electron ion recombination in dense plasmas, Phys Rev **125**, 795 (1962)

JUNE 1964 AIAA JOURNAL VOL 2, NO 6

Nonequilibrium Ionization Due to Electron Heating: II. Experiments

JACK L KERREBROCK* AND MYRON A HOFFMAN*

Massachusetts Institute of Technology, Cambridge, Mass

An experimental study has been conducted of nonequilibrium conductivity of mixtures of argon and potassium A pure plasma is produced in thermal equilibrium at temperatures up to 2500°K by means of a steady-flow tantalum heat exchanger Conductivity measurements made with probes between the electrodes indicate that the two-temperature conduction law proposed is valid for electron concentrations above about 10^{13} cm^{-3} The effective energy loss factor δ depends on the size of the apparatus and was found to be 10 for the test sections used in these experiments At lower electron concentrations, the theory is in error, probably because the electron energy distribution is very non-Maxwellian In this region, the electric field goes through a maximum with increasing current density, suggesting that it may be difficult to make the transition to the higher electron density nonequilibrium state from the initial low electron density equilibrium state in an MHD generator

Nomenclature

E = electric field, v/cm
E' = electric field as seen in the moving gas frame of reference
j = current density, amp/cm^2
k = Boltzmann constant
$\mathfrak{M}$ = molecular weight
$\dot{m}$ = mass flow rate, g/sec
S = collision cross section, cm^2
T = temperature, °K
V = voltage, v
α = slope, $(\partial \log\sigma/\partial \log j)_{T_a}$ (in two-temperature conduction law)
γ = slope, $(\partial \log\sigma/\partial \log T_a)_j$ (in two-temperature conduction law)
δ = energy loss parameter
σ = electrical conductivity, mho/cm

Subscripts

A = argon
a = gas (atom)
c = coulomb
e = electron
ex = excitation
K = potassium

Received October 31, 1963; revision received March 2, 1964 This study was supported by Air Force Office of Scientific Research Grant No 62-308 It was carried out under the auspices of the Research Laboratory of Electronics, Massachusetts Institute of Technology The authors are indebted to their colleague, Gordon C Oates, for many valuable discussions, and to Messrs Dethlefsen, Drouet, Larson, and Halstead, whose thesis work contributed greatly to the success of this study

* Associate Professor of Aeronautics and Astronautics Member AIAA

Introduction

THE theory of nonequilibrium conduction proposed in Ref 1, and further developed in Part I of this paper, was tentatively confirmed by experiments reported in Ref 1 Experiments reported in Ref 2, also, indicated reasonable agreement with the theory There were various uncertainties in these experiments, including purity and composition of the test gas, the uniformity of the current density, and electrode effects

The experiment to be described here was designed to eliminate these uncertainties and to determine the range of applicability of the proposed two-temperature conduction

law of Ref 1:

$$j/j^* = (T_a/T^*)^{\gamma/(1-\alpha)}(E'/E^*)^{1/(1-\alpha)}$$

where j^*, E^*, and T^* are reference conditions and where it is shown in Part I that γ and α are, in general, functions of both T_a and T for a given gas

It is of particular interest to determine that region over which γ and α can be assumed to be independent of T and, hence, functions only of the gas temperature T_a This leads to an especially simple and useful form of the two-temperature conduction law In addition, it is desired to determine what, if any, empirical corrections to the conduction law are necessary to permit it to be used for quantitative engineering calculations Therefore, the emphasis in the experimental work has been on the measurement and control of the thermodynamic condition and composition of the plasma to make it possible to determine accurately the relationship between its bulk conductivity and the current density

To insure the control of the composition and temperature of the plasma, it is produced in a continuous-flow heat exchanger, where it comes in contact only with stainless steel at the lower temperatures and tantalum at the higher temperatures This is particularly important, since a very slight contamination with polyatomic impurities could greatly influence the electronic energy loss The heat exchanger also insures the absence of extrathermal ionization in the plasma prior to its entrance to the test section Such residual ionization may be troublesome with arc heaters Finally, by designing the heat exchanger carefully, it has been possible to obtain a direct and accurate measurement of the plasma temperature

The conductivity has been determined by probe measurements between the electrodes, so that uncertainties due to electrode effects are eliminated Visual observation of the plasma has indicated that the current is quite uniformly distributed

In addition to these basic measurements, preliminary determinations of the excitation temperature of the first excited states of a trace impurity of sodium have been made by the classical line-reversal technique No great accuracy is claimed for these measurements; however, they do show a reasonable agreement with theory at high electron concentrations, where Maxwellization of the electrons is expected (see Part I)

All of the work to be reported here has been done with mixtures of argon and potassium The behavior of the conductivity, as predicted by the two-temperature conduction law, is shown in Fig 1 for the range of temperatures and

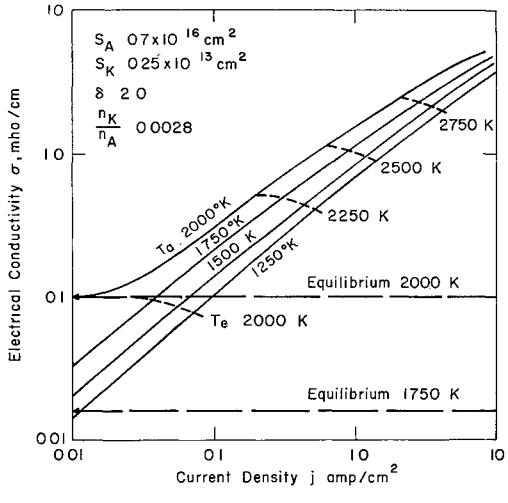

Fig 1 Theoretical variation of electrical conductivity with current density for various argon gas temperatures and for a potassium seeding fraction of 0 28%; total gas pressure is 1 atm

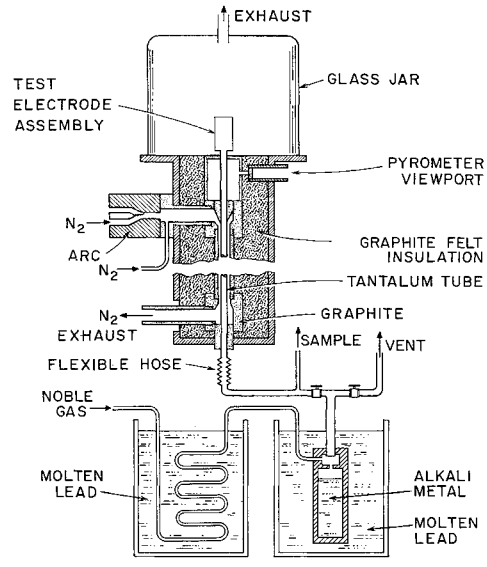

Fig 2 Experimental facility for generating pure noble gas-alkali metal plasmas at temperatures ranging from 1000° to 2500°K and 1 atm pressure

current densities attained in the experiments One point particularly should be noted The theory predicts that the slope of the lines of $\log\sigma$ vs $\log j$ (denoted α in Ref 1 and Part I of this paper) should be dependent only on the ratios of gas temperature to ionization energy and gas temperature to electron temperature If the electron temperature exceeds the gas temperature by more than about 10%, the predicted value of α is almost constant at about 0 8 This provides a rather sensitive check of the theory

Description of Test Facility

The test gas heater (Fig 2) is basically a counterflow heat exchanger A mixture of N_2 and A is heated by an arc source to several thousand degrees Kelvin and then flows down the annular region between a graphite outer tube and a $\frac{1}{4}$-in -diam tantalum inner tube and is exhausted as shown The graphite assembly is fixed only at the upper end, where it attaches to the arc, and is free to expand downward The tantalum tube is supported by a graphite sleeve at the top and is free to expand independently both above and below this sleeve With these provisions, the tantalum tube can be used for many runs, even though it becomes carburized and very brittle after the first run

A very pure test gas (welding grade argon with impurities of less than 30 ppm in the test to be described) is first put through a preheater consisting of a molten lead bath in a stainless-steel pot A stainless-steel potassium boiler (Fig 3) is immersed in a second pot, shown on the right in Fig 2 The temperature of this lead pot is carefully controlled at a constant value of about 850°C throughout the experiment This yields a vapor pressure of the liquid potassium of over 2 atm, resulting in choked flow through a 0 004- to 0 006-in -diam orifice at the top of the boiler The very low potassium flow rates, ranging from about 0 002 to 0 005 g/sec, required to obtain the desired seeding concentrations are obtained in this way

The argon mixes with the potassium vapor in the top of the potassium boiler, and the mixture flows into the tantalum tube at the base of the heat exchanger In order to vary the seed fraction during a run, the argon flow rate is varied To avoid disturbing the potassium boiler temperature, the argon preheater is separated from the boiler heater, as shown in Fig 2 Typical argon mass flow rates range from about 0 1 to 1 0 g/sec

The seeded test gas flows up through the tantalum tube in the counterflow heat exchanger and enters a test section

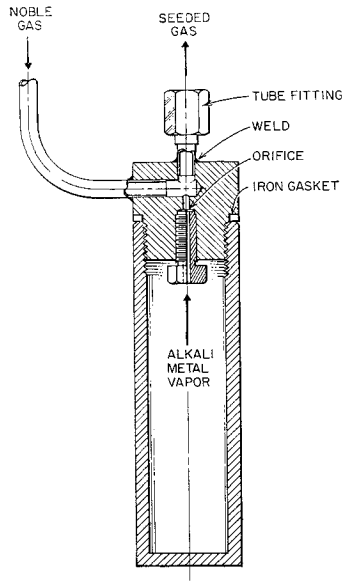

Fig 3 Stainless-steel boiler used for injecting very small, precise flows of alkali metal seed gases into noble gas flows

at any desired temperature between 1000° and 2500°K (depending primarily on the arc power) This results in flow velocities of at most about 100 m/sec in the test section

The entire heat exchanger is packed with graphite-felt insulation and supported in a steel pipe and frame assembly The insulation and the test section are purged with N_2 before and during each run to prevent oxidation of the high-temperature parts A pyrometer views the interior of a cavity which is essentially isothermal and through which the tantalum tube passes In this way, the gas temperature is measured within limits that will be given later

The test facility was designed to operate at up to 2500°K As many as five runs of about 3-hr duration each have been made at about 1500°K before any maintenance of the facility was required The normal maintenance required at this stage consists of replacement of the tantalum tube and possibly some of the smaller graphite parts connecting the arc assembly to the heat exchanger

This test facility can accommodate a wide variety of experiments with the minimum modification To date, five different test-section configurations have been employed on conductivity, electrode, and heat-transfer tests

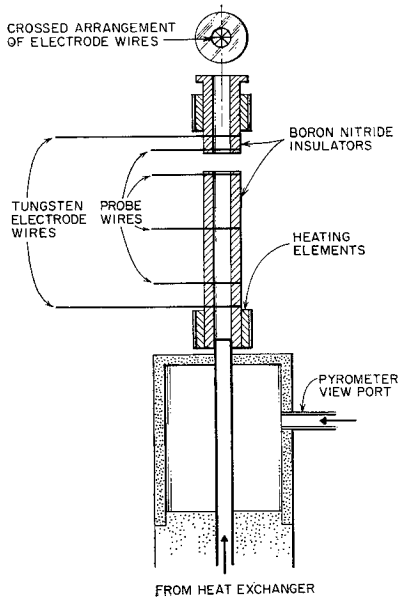

Fig 4 Test-section configuration 3A used to collect accurate bulk conductivity data for noble gas-alkali metal plasmas at gas temperatures from 1000° to 2000°K

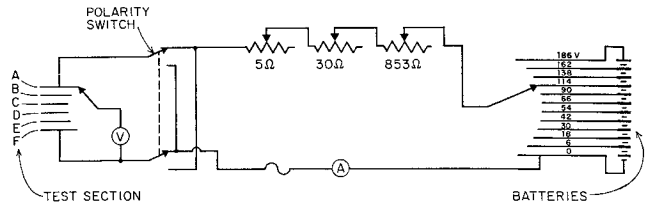

Fig 5 Wiring diagram showing test section, power supply, and electrical connections

Test Sections

The test-section configuration used to obtain the experimental results discussed in the next section is the result of considerable experience gained with other configurations in early tests [3,4] The three basic test-section configurations which have been tried in the conductivity experiments will be described briefly in order to bring out the principal features of the final configuration

All tests but those with the second configuration were run with the test section mounted on top of the heat-exchanger assembly as shown in Fig 2 The second configuration was mounted in the upper part of the heat exchanger in the open region near the pyrometer viewport

The first test-section configuration consisted of two circular tantalum electrodes mounted in a boron nitride insulator assembly Heater elements were incorporated in this assembly to insure that the gas would not cool excessively and that the potassium would not condense on the insulator walls The basic measurements included the voltage across the electrodes, the current (which flowed up or down the channel), and the various temperatures and gas flow rates

The results with this test section were very promising However, it was felt desirable to run a series of tests with the entire test section at the gas temperature, and so in the second configuration the insulator heaters were eliminated and the entire test assembly installed in the very hot upper part of the heat exchanger Circular tantalum electrodes were once again used, but, in addition, three tungsten probe wires were inserted across the test section to allow voltage measurements away from the electrode drop regions Two thermocouples were added to allow direct measurement of the gas and insulator temperatures

Several complicating factors arose with this arrangement The experimental results showed strange behavior up to current densities of about 1 amp-cm^{-2} which could possibly have been a result of some electrical conduction paths through the very hot boron nitride insulators (about 2000°K in some runs)

Therefore, the third test section, shown in Fig 4, was once again mounted on top of the heat exchanger, and nichrome wire heating elements were installed at the top and bottom The test-section insulator temperature was monitored continuously with a thermocouple

This test section incorporated all of the refinements evolved up to this point plus a gap in the boron nitride insulator This was inserted for two reasons First, it eliminates any insulator or wall-conduction paths across the gap Secondly, it permits direct observation of the uniformity of the plasma In addition, it allows direct measurements of electron "temperature" using the sodium line-reversal technique

This third test section configuration and mounting arrangement was the one used, with minor modifications of spacing and electrode configuration, in all of the tests to be discussed in this paper Each electrode consisted of four 0 015-in -diam tungsten wires arranged in a star or cross pattern across the channel Each probe consisted of a single 0 010-in -diam tungsten wire strung across the diameter of the test section at the appropriate location Three different arrangements of probe wires and gap location were tried All three variations gave essentially the same test results

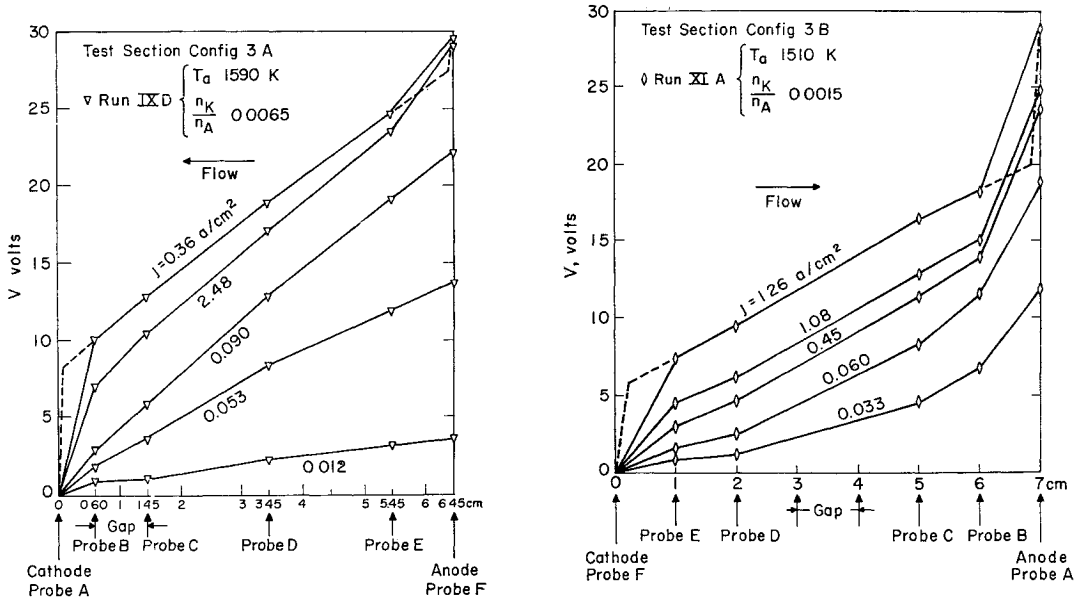

Fig 6 Typical experimental voltage variations along the test section both in the insulators and in the gap for two seeding fractions of 0 65 and 0 15% Note different polarities relative to the gas flow direction

The arrangement of the battery power supply, ballast resistors, and switches used to apply the voltage to the test section is shown in Fig 5 The test circuit was electrically isolated from the heat exchanger, so that no spurious currents could arise due to ground loops

Experimental Results

The basic experimental results are presented in this section, along with the general conclusions regarding their agreement with the two-temperature conduction law

Almost two dozen runs have been made with argon seeded with various mole fractions of potassium from about 0 1% to about 1% and over a range of gas temperatures from 1400° to about 2000°K Several of these runs are under almost identical conditions of temperature and seeding concentration and show excellent repeatability Four representative runs at about 1500°K gas temperature and four different seed fractions have been selected for detailed quantitative analysis in this paper The conclusions reached, however, are valid for all of the test results obtained to date

The basic electrical measurements in these experiments consisted of the voltages between the electrodes and each probe wire and the current flowing in the test section Direct plots of the voltages vs electrode and probe wire locations, such as those shown in Fig 6, yield the complete voltage variation in the test section for each current density

Using these results, it is possible to separate clearly the volume characteristics of the plasma from the electrode surface and electrode drop effects All conductivity calculations presented in this paper are based on the average electric field in the gas well away from the electrodes

It should be noted that the electric field between probe wires in the boron nitride insulator is essentially the same as that in the gap, except at the lowest current densities It is observed that the electric field tends to increase, and hence the electrical conductivity tends to decrease, as the gas flows from the bottom to the top of the test section for the lower current densities This is true for both polarities of the bottom electrode and is most probably due to a slight cooling of the plasma by radiation and conduction At the higher current densities, joule heating tends to counter these losses, and the electric field tends to decrease less with distance along the test section

The important conclusion to be drawn from these voltage profiles is that the conductivities calculated from the electric field in the insulators and in the gap are essentially the same In addition, they are clearly free of electrode effects

The electrode drops can be seen to range from almost zero up to about 10 v for the higher current densities Note that straight lines have been drawn between data points, but that some dotted lines have been included to suggest that the electrode drops may actually occur in a shorter distance No further interpretation of the electrode effects will be included in this paper, since the electrode geometry in these test sections was not well suited to analysis Special electrode investigations are underway with more suitable geometries and will be reported in the near future

The experimental electric field vs current density characteristics for the four representative runs are shown in Fig 7 These characteristics definitely have the shape predicted by the two-temperature conduction law at the higher current densities, but they fall above the theoretical curves for $\delta = 2\ 0$

A transition region is apparent at the low current densities where a peak in required electric field occurs A possible explanation of this will be given in the next section

The corresponding conductivity curves are shown in Fig 8 for the same gas temperatures and seeding fractions These

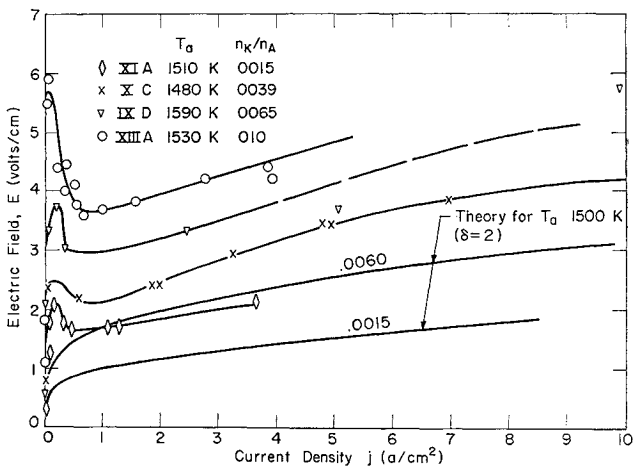

Fig 7 Experimental electric field vs current density characteristics for four different seeding fractions but all at about 1500°K gas temperature using an argon gas seeded with potassium at 1 atm total pressure

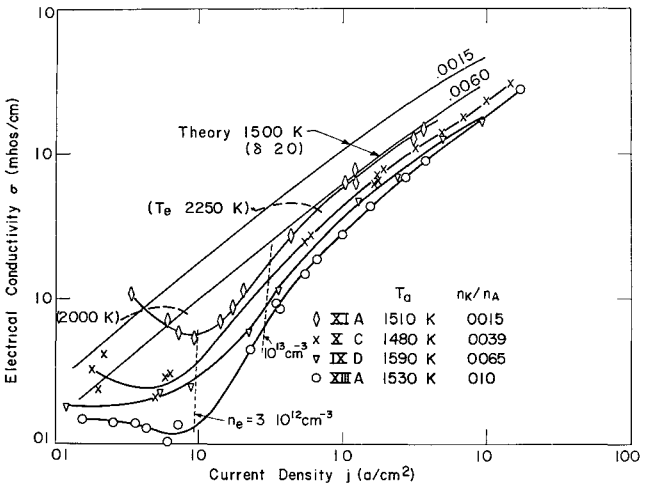

Fig 8 Comparison of theoretical and experimental conductivity vs current density curves for the four experimental runs of Fig 7

represent runs made over a period of many months during which time excellent reproducibility of the results was obtained above about 0 3 amp/cm² Below this level, the transition region corresponding to the hump in the voltage-current characteristics of Fig 7 varied somewhat from run to run It should be noted that the peaks of the voltage-current characteristics of Fig 7 correspond to the region near the minimum conductivity points of Fig 8

From the practical viewpoint, the low current density data are very important in one particular respect They indicate that the electric field in the plasma must rise above its final value as the plasma passes from the equilibrium to the nonequilibrium state Since, in some practical MHD devices such as generators, the electric field is limited by the product of flow velocity and magnetic field, it may be difficult to attain the desired operating point

Comparison with Theory

In order to facilitate comparison of the theory and the experimental runs at different potassium seeding fractions, it is useful to change variables so as to eliminate dependence on n_K/n_A Based on the theory, this can be achieved by using normalized values of j and σ defined as follows:

$$\tilde{j} \equiv j \left[\frac{(n_K/n_A)_{ref}}{(n_K/n_A)} \right]^{1/2}$$

$$\tilde{\sigma} \equiv \sigma \left[\frac{(n_K/n_A)_{ref}}{(n_K/n_A)} \right]^{1/2} \frac{[1 + (n_K/n_A)(S_K/S_A)]}{[1 + (n_K/n_A)_{ref}(S_K/S_A)]}$$

A convenient and meaningful reference value for n_K/n_A is the optimum seeding fraction at a constant electron temperature In order to find the optimum value of the seeding fraction, the conductivity equation can be differentiated with respect to seeding fraction holding T constant This leads to the result that $(n_K/n_A)_{opt} = S_A/S_K$

As a first estimate to facilitate normalization, constant values of $S_A = 0\,7 \times 10^{-16}$ cm² and $S_K = 0\,25 \times 10^{-13}$ cm² have been selected, giving $(n_K/n_A)_{pt} = 0\,0028$

Table 1 Estimated errors in the basic variables

	Estimated errors
Conductivity σ	± 9%
Potassium mole fraction n_K/n_A	± 12%
Gas temperature T_a	± 50°C
Potassium excitation temperature T_x	±100°C

The normalized j is theoretically a function only of the gas temperature and pressure, the seed gas ionization energy, the energy loss parameter δ, and the electron temperature in regions where hard sphere collisions dominate For the same experimental conditions of gas temperature and pressure, all experimental points at the same electron temperature should fall at the same value of $\tilde{j}$

Similarly, the normalized σ is a function only of the gas pressure, the argon collision cross section, the seed gas ionization energy, and the electron temperature Therefore, all experimental points at the same electron temperature should fall at the same value of $\tilde{\sigma}$ As a result, on a plot of $\log\tilde{\sigma}$ vs $\log\tilde{j}$, all experimental points should fall on a single curve, in the region where hard sphere collisions dominate

The normalized conductivity curves are shown in Fig 9 The theoretical curves all fall exactly on a single curve in the region shown

The experimental curves fall remarkably close to a single curve at the higher current densities, leading to several important general conclusions First is that the theory predicts the correct variation of conductivity with current density above about 0 3 amp-cm^{-2} In this region, it can be seen that the experimental slopes α are very close to those predicted theoretically, providing strong support for the two-temperature conduction law In addition, these results indicate that the average collision cross sections selected for argon and potassium are reasonably valid, and that the measured values of (n_K/n_A) are quite accurate

A detailed error analysis is given in the Appendix The estimated errors in the basic variables are collected in Table 1 Comparison of these estimates with the experimental results in Fig 9 indicates that the over-all accuracy is, in fact, better than these estimates would indicate

The major discrepancy between the theory and the experimental results for the higher current density region is that the experimental conductivities are consistently about one-half the theoretical values If we adjust δ to a value of about 10, the agreement is then excellent, as shown in Fig 9

There are several possible explanations for this apparent increase in the electronic energy loss The most obvious is impurities in the test gas This is ruled out on the grounds that the impurity level of the welding-grade argon is too low to be significant, whereas the excellent reproducibility of the results virtually eliminates the possibility that contamination is significant

The most probable explanation of the increase in δ is that the electron gas loses energy by radiation Estimates of this energy loss have been made by Byron[5] and by Lutz[6] The most that can be said at the present time is that the pre-

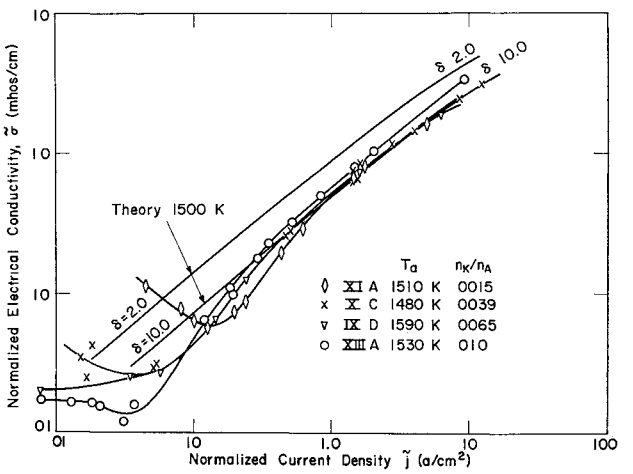

Fig 9 Normalized conductivity vs current density curves for the four experimental runs of Fig 8 Note that a theoretical curve for a δ = 10 is the best fit to the data

dicted energy losses are of the right order to explain a δ of 10 in apparatus of the present size If this is the correct explanation, then the effective δ should approach 2 as the size of the apparatus increases or as the optical density of the plasma increases

Close examination of Fig 9 shows that, indeed, the curve for $n_K/n_A = 0\,01$ does have a higher slope than the curves for lower potassium concentrations It is tempting to attribute this to the greater optical density that results from the larger potassium concentration; however, there are other factors that could explain the trend Among these are joule heating of the gas and the variation of collision cross sections with electron energy (e g , Ref 7) The question could be resolved by a direct measurement of the intensity of the emitted radiation

For lower current densities, the experimental results de part substantially from the theory As the electric field is raised from zero to a few tenths of a volt per centimeter, an unexpectedly large current flows in the region near the origin of Fig 7 This corresponds to the anomalously high conductivities of Fig 8 at very low current densities of about 0 01 to 0 10 amp-cm^{-2} No explanation can be offered for this behavior at the present time

As the electric field is raised further to values of one or more volts per centimeter, the current density does not increase as rapidly as the theory predicts As a result, in the region from 0 1 to about 0 3 amp-cm^{-2}, the conductivity is depressed below the theoretical values It is very likely that, in this region, the electrons have not yet achieved a Maxwell-Boltzmann distribution As the current density is raised from zero, the high-energy tail is depleted faster than it can be filled because ionization must be done by these more energetic electrons The low electron-electron collision frequencies at these low current densities prevent the electron density from building up as fast as the theory predicts Thus, the electric field required to pass a given current density would rise above the theoretical values, as indicated by the hump in Fig 7

We expect a Maxwellian distribution when

$$n\,^2S \gg \delta(m/m_a)n\,(n_AS_A + n_KS_K)$$

The electron energies most important for ionization are about 2 ev, where $S \approx 10^{-13}$, $S_A \approx 10^{-15}$, and $S_K \approx 3 \times 10^{-14}$ cm^2 Using $\delta = 10$ and $m/m_a \approx 10^{-5}$ leads to the requirement that $n/n_a \gg 10^{-6}$ for Maxwellization of the electrons For typical seeding fractions, $n_K/n_A \approx 0\,003$, and at atmospheric pressure and 1500°K gas temperature, the criterion implies a required electron concentration, $n \gg 5 \times 10^{12}$ cm^{-3}

Calculation of the electron densities using the experimental results yields lines of constant electron density as indicated in Fig 8 The line of electron density equal to 10^{13} cm^{-3} falls very close to $j = 0\,3$ amp-cm^{-2}, where the transition can be seen to occur

This close correspondence between the theoretical predictions of the transition n of Part I of this paper and the experimental results lends weight to the theory that the non-Maxwellian distribution of the electrons contributes to the anomalous behavior observed at low current densities

Initial attempts to measure electron temperature directly employed the sodium line-reversal technique using the standard arrangement shown in Fig 10 [8-10] The temperature at which the sodium D line is reversed is assumed to be a measure of the excitation temperature of the first excited state of the sodium atoms This will be equal to the electron temperature if the electron-electron collision frequency is high enough to result in the attainment of equilibrium for the entire electron gas

Line reversal was obtained only up to excitation temperatures of about 2600°K, since the tungsten strip-lamp light source used limited the maximum effective source tempera-

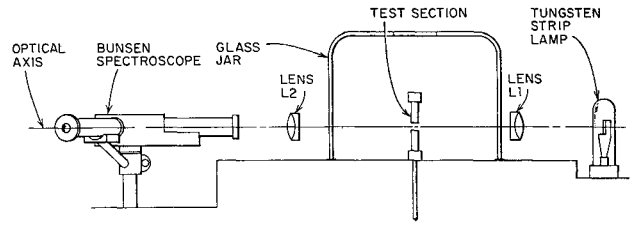

Fig 10 Line reversal apparatus used to measure excitation temperature in the test-section gaps of a trace of sodium added to the argon-potassium flow

ture to about this value Thus, most of these measurements are in the low current density transition region

The basic excitation temperature measurements, corrected for optical path and color effects, are shown by the solid lines in Fig 11 These measurements indicate a strongly elevated excitation temperature and lend support to the two-temperature conduction law However, it is apparent that the measured excitation temperature differs somewhat from the electron temperature predicted by theory

The possible effect of a radial variation of the current density is also shown in Fig 11 by the dashed curves A parabolic gas temperature variation across the test section was assumed, and the corresponding current density variation was calculated based on the two-temperature conduction law The resulting current density variation yielded a ratio of the maximum j to the average j of about 2 0 for a wall temperature 1000°C below the peak temperature in the center of the jet It is possible that the higher electron temperature region dominates when a region of the gas with temperature variations is examined spectroscopically [11] Therefore, the dashed curves in Fig 11 incorporate a correction, assuming that the effective j is twice the average value based on the test-section cross-sectional area As such, these dashed curves represent the maximum reasonable shift to the right of the experimental data

In general, the measurements of excitation temperature support the foregoing argument about the transition region, in that they show a rapid rise of excitation temperature in the range of current densities where the electrons should begin to Maxwellize It should be noted that, at a low current density of 0 01 amp-cm^{-2}, the measured excitation temperature is close to the gas temperature, but the conductivity (and hence n) is much larger than it should be in equilibrium It is undoubtedly true that much more work would be required to achieve an understanding of the plasma behavior at these low electron densities

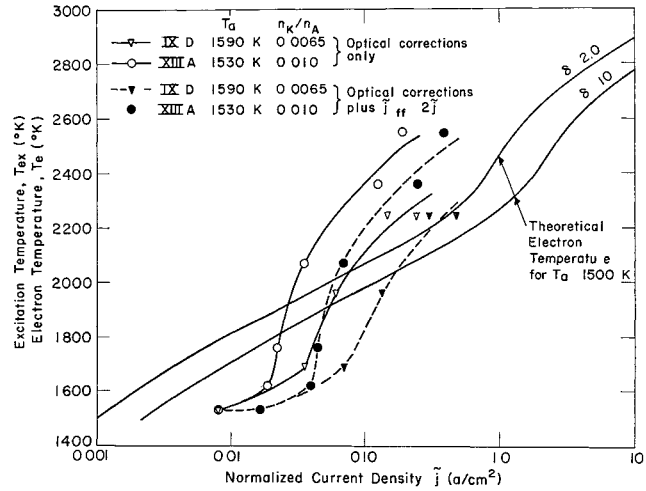

Fig 11 Preliminary sodium excitation temperature measurements compared to theoretical electron temperatures as a function of the normalized current density

Conclusions

It is concluded from the previously given evidence that the two-temperature conduction law provides a satisfactory description of the behavior of a noble gas-alkali metal plasma at electron concentrations greater than about 10^{13} cm^{-3}, in the absence of a magnetic field

For argon and potassium mixtures in apparatus with a 1-cm-length scale, the effective energy loss parameter δ is about 10 rather than the ideal value of 2 It seems likely that this increase is due to radiative energy loss, so that the effective δ should be smaller in larger apparatus

At low electron concentrations, the simple theory is inadequate, probably because the electrons have a highly non-Maxwellian energy distribution The electric field required to produce a current in the plasma displays a maximum value as the current is increased from very low values This suggests that, in applications such as the MHD generator, there may be difficulty in passing from the equilibrium state of the plasma at entry to the desired nonequilibrium state in the generator

As noted in Part I, there seems to be no reason to doubt that the relationship between conductivity and current density verified here will also apply in magnetic fields However, the question of instabilities does arise at large values of the Hall parameter These questions are currently being studied experimentally in a modified version of the apparatus just described

Appendix: Analysis of Measurement Techniques

The basic electrical measurements consisted of the voltages between the electrodes and each probe wire, and the current through the test section These were measured using Hewlett-Packard 412A vacuum tube voltmeters, which have a full-scale accuracy of $\pm 3\%$ The electrode and probe wire locations were known to within about $\pm\frac{1}{4}$ mm or within ± 2–3%

The electric field E used in Fig 7 is based on the average value in the gas between probes B and E Based on the foregoing figures, this average electric field is estimated to have an inaccuracy of about $\pm 6\%$, attributable primarily to the Hewlett-Packard 412A

The current density j is computed from the ratio of the total current to the cross-sectional area of the test-section flow passage It was observed in all runs that a diffuse plasma flowed through the gap in the test section Hence, the current density based on the area of the flow passage represents a good average value When the expected radial temperature variation for laminar pipe flow is taken into account, the average value differs from the maximum value of current density in the center of the flow by at most a factor of 2 Ignoring the radial variation of the current density across the test section, the estimated inaccuracy in the average value of the current density is about $\pm 6\%$ This is due primarily to the stated inaccuracy in the Hewlett-Packard 412A used as an ammeter

It can be seen that the combined inaccuracies in both E and j are not large enough to change the basic shape of the voltage-current characteristics of Fig 7 In fact, the scatter in the data points is probably a good indication of the effect of varying inaccuracies on different scales of the vacuum tube voltmeters The scatter is approximately equal to the inaccuracy estimates previously mentioned

The electrical conductivity σ is calculated from Ohm's law and is equal to the ratio of the average current density j and the average field E The inaccuracies in E and j carry over in the calculation of σ Random inaccuracies in E would tend to show up as scatter of the data points This amount of scatter does show up in Fig 8 However, random inaccuracies in j would tend to shift the data points up or down along the experimental curve at the higher current densities, since the slope of the curve is close to unity This would tend to cancel out the effect of random j inaccuracies on the $\log\sigma$ vs $\log j$ plot above about 0 3 amp-cm^{-2}

Although the random inaccuracies in E and j can be seen to have only a second-order effect on the experimental conductivity curves, errors in the estimation of either the gas temperature T_a or the seeding fraction n_K/n_A can have a first-order effect That is, errors in T_a or n_K/n_A will be manifested as a systematic shift or deviation of the experimental curve from the theory It is, therefore, vitally important to have an accurate estimate of these inaccuracies

The gas temperatures were inferred from measurements of the temperature of the cavity at the top end of the heat exchanger (see Fig 2) using a Leeds and Northrop optical pyrometer Earlier tests using a tungsten-rhenium thermocouple inserted directly into the plasma in the test section revealed that the thermocouple temperature was about 50°C below the pyrometer temperature This empirical correction was included in the gas temperature values quoted

The error in this empirical correction is difficult to estimate, since the emissivity of the thermocouple is not known The calibration of the tungsten-rhenium thermocouple was given to $\pm 2\%$ or $\pm 30°$–$40°$ Thus it is felt that the gas temperatures are within ± 50°C of the quoted values

Based on the two-temperature conduction law, a systematic error of 50°C in the gas temperature would shift the conductivity curves of Fig 8 by about 6–10% at the low current densities and by about 4–6% at the high current densities This would be a small but noticeable shift in the $\log\sigma$ vs $\log j$ curves

The mole fraction of potassium is calculated from the following equation:

$$\frac{n_K}{n_A} = \frac{\dot{m}_K}{\dot{m}_A} \times \frac{\mathfrak{M}_A}{\mathfrak{M}_K} \approx \frac{\dot{m}_K}{\dot{m}_A}$$

since the molecular weights of argon and potassium are essentially the same

The potassium mass flow rate estimate was based primarily on the average value computed from the total weight of potassium loaded in the boiler and the total run duration The potassium boiler was maintained at constant temperature throughout the run to within ± 4°C This should result in about $\pm 3\%$ variation in mass flow rate through the choked orifice of the boiler The major inaccuracy is due to the uncertainty in the estimate of the run duration which was about ± 15 min or about $\pm 10\%$ of the average run duration

The argon flow rate was measured with a Fisher-Porter flowmeter of the spherical-float-in-a-tapered-tube type This has an accuracy of $\pm 3\%$ of full scale, resulting in average errors around $\pm 6\%$ for flows around half scale

The over-all inaccuracy in the calculation of the potassium mole fraction is taken as the square root of the sum of the squares of the inaccuracies of each of the independent error sources This results in an estimated inaccuracy of $\pm 12\%$ in the mole fraction estimate Based on the theory, a systematic error in n_K/n_A of $+12\%$ would shift the conductivity curves of Fig 8 by about -6%

Comparing this shift in the conductivity curves with the shift due to gas temperature errors, it can be seen that an error in mole fraction of 12% has approximately the same effect on the conductivity curves as an error in gas temperature of about 50°C These two sources of error are, therefore, of about equal importance in causing small but noticeable shifts in the conductivity curves (Fig 8) Thus, it is not possible to separate the effects of these two error sources at this time However, the total effect is seen to be well within the previously given inaccuracy estimates from Figs 8 and 9

The excitation temperature was measured using the standard sodium line-reversal technique employing the optical arrangement of Fig 10 The tungsten strip lamp tempera-

ture was calibrated using an optical pyrometer, and appropriate color and optical path corrections were made (see, e g , Refs 8–10) The optical path correction was determined by first calibrating the lamp alone and then recalibrating through the first lens and glass jar This was a very important contribution to the optical corrections, amounting to over 5% reduction in effective lamp temperature due to the low optical quality of the bell jar and lens The over-all optical corrections ranged from about 100°C at the low electron temperatures up to over 200°C at the high electron temperatures The corrected values are the solid curves shown in Fig 11

There were several uncertainties in the excitation temperature measurements The principal one was the range of lamp temperatures over which reversal occurred The sodium D line would start reversing at the top of the image (corresponding to the top of the gap in the test section) The line would not be completely reversed, however, until the temperature of the lamp was raised about 200°C higher The data points plotted are average values corresponding to half the line reversed This leads to an uncertainty on order of ± 100°C for the excitation temperature in the gap Other errors due to pyrometer calibration and reading uncertainties were much smaller than this figure

References

[1] Kerrebrock, J L , ' Conduction in gases with elevated electron temperature," *Engineering Aspects of Magnetohydrodynamics* (Columbia University Press, New York, 1962), pp 327–346

[2] Robben, F , "Nonequilibrium ionization in a magnetohydrodynamic generator," Phys Fluids **5,** 1308–1309 (1962)

[3] Dethlefsen, R and Drouet, M , "Measurement of electrical conductivity in non equilibrium argon-potassium plasma," S M Thesis, Massachusetts Institute of Technology (August 1962)

[4] Halstead, F C and Larson, E L , "Experimental determination of the electrical conductivity of noble gas-alkali metal plasmas," S M Thesis, Massachusetts Institute of Technology (August 1963)

[5] Byron, S , Bortz, P I , and Russell, G R , "Electron-ion reaction rate theory," *Proceedings of the Fourth Symposium on the Engineering Aspects of Magnetohydrodynamics* (University of California Press, Berkeley, Calif , 1963), pp 93–97

[6] Lutz, M , "Radiant energy loss from a cesium argon plasma to an infinite plane-parallel enclosure, ' Avco Everett Research Lab , Res Rept 175 (September 1963)

[7] Brown, S C , *Basic Data of Plasma Physics* (John Wiley and Sons, Inc , New York, 1959), Chap 1

[8] Jones, G W Lewis, B , Friauf, J B , and Perrott, G , "Flame temperatures of hydrocarbon gases," J Am Chem Soc **53,** 869–873 (1931)

[9] Lewis, B and Von Elbe, G , "Flame temperature," *Temperature—Its Measurement and Control* (American Institute of Physics, New York, 1941), Vol 1, Chap 8

[10] Gaydon, A G and Wolfhard, H G , *Flames, Their Structure, Radiation and Temperature* (Chapman and Hall, London, England, 1960), Chap 10

[11] Strong, H M and Bundy, F P , "Measurement of temperatures in flames of complex structure by resonance line radiation," J Appl Phys **25,** 1521–1530 (1954)